JOURNAL OF PROPULSION AND POWER
Vol. 12, No. 4, July–August 1996

Wave Rotor Optimization for Gas Turbine Engine Topping Cycles

Jack Wilson*
NYMA, Inc., Brook Park, Ohio 44142
and
Daniel E. Paxson†
NASA Lewis Research Center, Cleveland, Ohio 44135

Use of a wave rotor as a topping cycle for a gas turbine engine can improve specific power and reduce specific fuel consumption. Maximum improvement requires the wave rotor to be optimized for best performance at the mass flow of the engine. The optimization is a tradeoff between losses because of friction and passage opening time and rotational effects. An experimentally validated, one-dimensional computational fluid dynamics code, which includes these effects, has been used to calculate wave rotor performance and find the optimum configuration. The technique is described, and results given, for wave rotors sized for engines with sea level mass flows of 4, 26, and 400 lb/s.

Nomenclature

A = total wave rotor inlet area from the compressor
A_n = area of a single wave rotor inlet, A/n
a^* = reference speed of sound, in passage just prior to opening to exhaust
b = wave rotor passage width
c_{p1} = specific heat of air before entering the combustor
c_{p4} = specific heat of gas after leaving the combustor
D_h = passage hydraulic diameter
e = difference between inlet and exhaust mass flow rate used in Eq. (4)
f = friction factor
G = leakage parameter, $2\delta/h$
h = wave rotor passage height
L = wave rotor passage length
$\dot{m}$ = engine mass flow
n = number of cycles on the wave rotor
P_i = stagnation pressure at port i
p_i = static pressure at port i
R = rotor radius at midpassage height
T_i = stagnation temperature at port i
t = time
U = axial flow velocity at input to rotor
u = velocity inside a passage
W = circumferential velocity of rotor
γ = specific heat ratio for combustion gases
δ = spacing between rotor and end-wall
ε = expansion ratio, ratio of p_4 to pressure in passage before opening to the exhaust port 4
μ = viscosity
Π_s = shaft compression ratio, i.e., P_1/P_0, which is the compression ratio of the mechanical compressor
ρ = density at input to rotor
ρ^* = reference density, i.e., density in passage just prior to opening to exhaust port 4
τ = nondimensional time, ta^*/L
τ_{cycle} = nondimensional time for one cycle
τ_{in} = nondimensional time inlet port is open
τ_{ot} = nondimensional passage opening time
ϕ_{in} = angle subtended by inlet port
ω = rotor angular velocity, rad/s

Subscripts
N = last computational cell
0 = first computational cell, also ambient conditions for engine
1, 2, 3, 4 = wave rotor ports indicated in Fig. 1

Introduction

A WAVE rotor is a machine in which air is pressurized in shock waves or compression waves, and expanded in unsteady expansion waves, within a single device. Basically, a wave rotor consists of a rotating bank of passages, inside a housing, with ports bringing air in or taking air out (Fig. 1). It is not a new device, having been invented by Seippel in 1940 (Ref. 1), with an intended application as a topping cycle for gas turbine engines. It has proved remarkably versatile, having also found application as a supercharger for automobiles,[2–5] as a source of air at very high pressure and temperature for a hypersonic wind tunnel,[6] as an air conditioner for mines,[7] and as a complete engine.[8,9] The performance of a wave rotor configured as a topping cycle for ground-based power units was demonstrated in a recent experiment.[10] This experiment showed that large improvements in efficiency and power are possible. In the configuration used in Ref. 10, the additional power created by the use of a wave rotor was extracted by a separate power turbine, using air tapped from the high-pressure port 2 (Fig. 1). This is appropriate for ground-based units used for generating electrical power, but would require large changes if applied to an aircraft engine. For an aircraft gas turbine, at least for an initial demonstration, it is desirable to use a different cycle; one in which the extra power is manifested as an increase in pressure at the exhaust port 4. Using this cycle, the wave rotor can be retrofitted into an existing aircraft gas turbine engine without using an extra power turbine. Such cycles have been tested by Klapproth et al.,[11] and Ruffles.[12] The objective of this work is to estimate the increases in specific power, and reductions in specific fuel consumption that could be achieved by retrofitting this type of wave rotor topping cycle into an existing aircraft gas turbine

Received June 12, 1995; revision received Dec. 27, 1995; accepted for publication Jan. 31, 1996. This paper is declared a work of the U.S. Government and is not subject to copyright protection in the United States.

*Senior Engineering Specialist, 2001 Aerospace Parkway. Senior Member AIAA.
†Aerospace Engineer, 21000 Brookpark Road. Member AIAA.

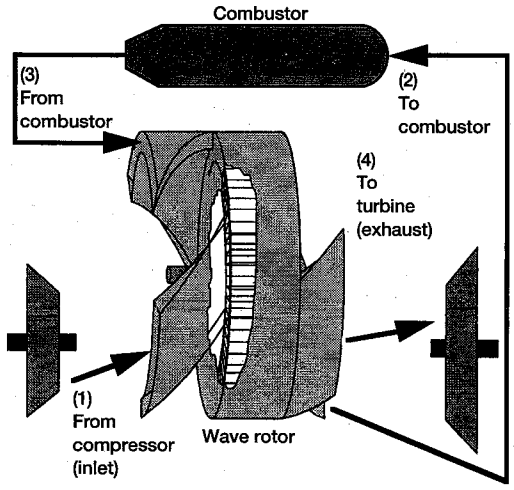

Fig. 1 Schematic diagram of a four-port wave rotor.

engine. Future application may involve wave rotors in which combustion takes place onboard the rotor,[9,13] possibly permitting even greater improvements in performance.

With a wave rotor installed as a topping cycle in a gas turbine engine, the air from the engine compressor would be directed into the wave rotor at the input port 1 (Fig. 1). The air flows into the passages on the rotor, and is compressed by a series of compression or shock waves. This air leaves the wave rotor from port 2, at a higher pressure than when it entered the wave rotor, and passes to the burner. After being heated in the burner, the gas returns to the wave rotor through port 3, driving a shock into the air in the passages in the process. This gas is trapped onboard as port 3 closes, at quite high pressure. When the rotor comes around to exit port 4, the gas expands out into the lower static pressure in the port. From there the gas goes to the engine turbine. In passing through the wave rotor, the air is first compressed and then expanded. Thus, the wave rotor combines, in a single device, the functions performed by the compressor and turbine in a high spool. By using a wave rotor topping cycle, combustion temperatures greater than the turbine inlet temperature can be used, since the gas leaving the combustor is cooled in the expansion before being sent to the turbine. Also, since the rotor is washed alternately by cool inlet air and hot combustion gas, it is self-cooled, and attains a steady-state temperature significantly lower than the combustion temperature. By increasing the overall cycle pressure ratio, and allowing higher combustion temperatures, the wave rotor topping cycle offers a potential route to higher engine efficiency.

The successful application of a wave rotor topping cycle is dependent upon how much performance improvement it can achieve over a conventional cycle. Calculations of improvements in specific power and efficiency have been reported.[14] In making such calculations, it is necessary to know the performance of the wave rotor. What is meant by wave rotor performance is the pressure gain created by the wave rotor as a function of the temperature ratio across it, i.e., P_4/P_1 vs T_4/T_1. Note that this pressure gain, P_4/P_1, is equivalent to the pressure at the exit of a turbine divided by the pressure at the entrance to the compressor. It should not be confused with the compression ratio, which is commonly used as a measure of performance in gas turbine engine cycles. In Ref. 14, the wave rotor pressure gain was taken to be that measured by Klapproth et al.[11] This is a conservative assumption, in that this performance has clearly been demonstrated, but has certainly not been optimized. The better the performance of the wave rotor, the greater the increase in specific power, and reduction in specific fuel consumption of the engine/wave rotor combination. The wave rotor performance will depend on the losses, which in turn depend on the geometry, and inlet conditions, of the wave rotor. What is needed then is a realistic calculation of wave rotor performance, including the major losses, which can be used to examine variations in geometry to find optimum performance. A suitable, one-dimensional, computational fluid dynamics (CFD) code has been written,[15,16] and was used for this report. The code has been validated against experiment,[17] and gives good agreement with the experimental results of Klapproth et al.,[11] and Kentfield.[18] Using this code, an optimum wave rotor size has been found for hypothetical engines with mass flows typical of small, medium, and large gas turbine engines. Finally, the specific power and specific fuel consumption of these engines was calculated assuming a wave rotor topping cycle employing the optimized wave rotor, for comparison with the basic engine.

Advantages of Using a Wave Rotor

The thermodynamic advantages of using a wave rotor topping cycle can be calculated with a simple model.[14] The details of the calculation are standard, and will not be repeated here. The advantages are precisely the same as would be found for a topping cycle composed of a conventional compressor and combustor and turbine combination, from which no net shaft work is extracted.

It will be assumed that for the basic engine, the value of $\Pi_s = P_1/P_0$ is known. The turbine inlet temperature and the compression and turbine efficiencies are also assumed known. With these quantities given, the specific power and specific fuel consumption of the basic engine can be calculated. When a wave rotor topping stage is added, it will be assumed that the turbine inlet temperature remains unchanged, but the pressure entering the turbine is raised from P_1 to P_4. Thus, to calculate the performance in this case, it is necessary to know the pressure ratio P_4/P_1 generated by the wave rotor for a given temperature ratio across it, i.e., T_4/T_1. The temperature ratio T_4/T_1 is fixed by the engine's turbine inlet temperature and compressor exit temperature.

The wave rotor pressure ratio as a function of the wave rotor temperature ratio is not a unique function. It depends on the geometry of the wave rotor, which will change with the mass flow of the engine, and on the expansion ratio used. In Ref. 14, a fit to the results of Klapproth et al.[11] was used. As explained previously, use of this fit is conservative; the performance should be amenable to improvement, since the experimental rotor was neither well timed, nor optimized. Moreover, the experimental rotor had a small mass flow; in general, wave rotor performance improves as the mass flow increases. The curve-fit to the experimental results was obtained using the one-dimensional CFD code described later, with estimates of the geometry of the rotor, to calculate the wave rotor pressure ratio at different values of the wave rotor temperature ratio. The fitted curve is the line shown in Fig. 2. Also shown are the experimental points from Ref. 1, which are the solid circles. Although the fit to the experimental points appears to be quite good, this must be regarded as somewhat fortuitous. The timing (i.e., when the ports open and close) of the experimental rotor was not known, neither was the exact geometry, nor the size of any leakage gaps. Consequently, an exact calculation was not possible. Nevertheless, the fit is obviously of the right magnitude, and should provide a good estimate of the wave rotor performance for this rotor.

With the wave rotor pressure ratio known from Fig. 2, the specific power, thermal efficiency, and specific fuel consumption can be calculated. In Ref. 14, calculations of the thermal efficiency of an untopped engine, calculated as previously discussed, were compared with results from the ONX program,[19] and found to give excellent agreement, giving confidence in this approach.

With this model, and the curve-fit to the data of Ref. 11, values of specific power, and specific fuel consumption have been calculated for shaft compression ratios (i.e., the compression ratio of the mechanical compressor) between 5–50,

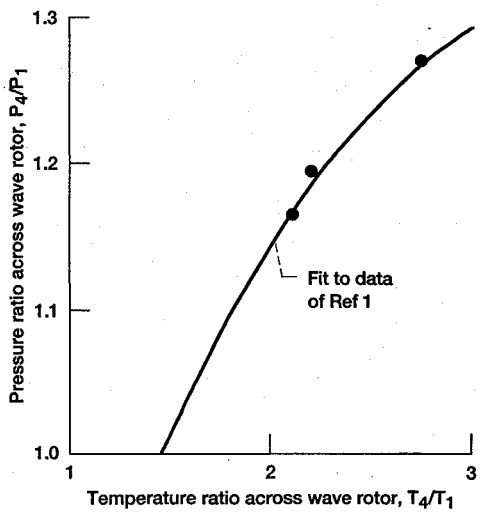

Fig. 2 Wave rotor performance measured experimentally by Klapproth et al.[11] (•), together with a curve-fit calculated with the CFD code (——).

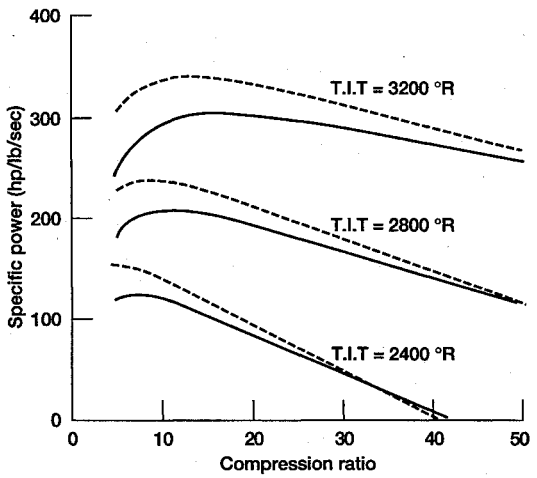

Fig. 3 Specific power vs shaft compression ratio for engines with (----) and without (——) a wave rotor topping cycle.

for engines with, and without, a wave rotor topping cycle. Turbine inlet temperatures of 2400°R, typical of a small engine, and 2800 and 3200°R, appropriate for an advanced engine, were used. Sea level ambient conditions were assumed. The results are shown in Figs. 3 and 4. It can be seen that quite large increases in specific power are possible by the addition of a wave rotor topping cycle, particularly at low values of the shaft compression ratio. For example, at a turbine inlet temperature of 2400°R and a shaft compression ratio of 8, addition of a wave rotor topping cycle increases the specific power by 19.2%, and reduces the specific fuel consumption by 16.2%. Raising the turbine inlet temperature to 3200°R at a compression ratio of 8 reduces the gain. At these conditions, the specific power increases 17.4%, and the specific fuel consumption decreases by 14.8%. Increasing the compression ratio reduces the gain even more dramatically. At a shaft compression ratio of 40, the specific power increase is 5.8%, and the specific fuel consumption decrease is 5.6%. An engine with a turbine inlet temperature of 2400°R and a compression ratio of 40 would actually decrease its performance by the addition of a wave rotor topping cycle. However, neither an engine with a shaft compression ratio of 8 and a turbine inlet temperature of 3200°R, nor an engine with a shaft compression ratio of 40 and a turbine inlet temperature of 2400°R, are well-designed engines; an actual engine is more likely to have a compression ratio somewhere between the value giving the minimum specific fuel consumption, and the value giving the maximum specific power for the turbine inlet temperature of that particular engine. The actual value is strongly influenced by the mission requirements of the engine.

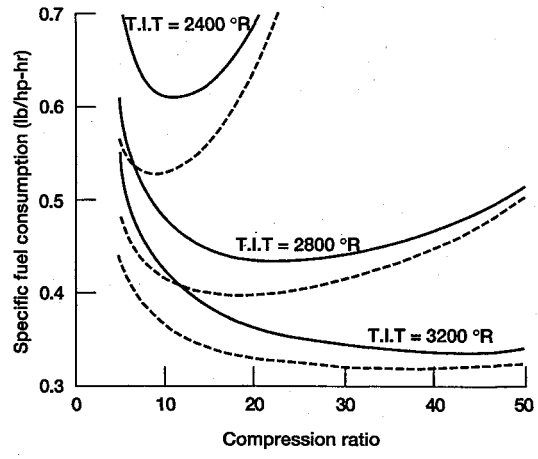

Fig. 4 Specific fuel consumption vs shaft compression ratio for engines with (----) and without (——) a wave rotor topping cycle.

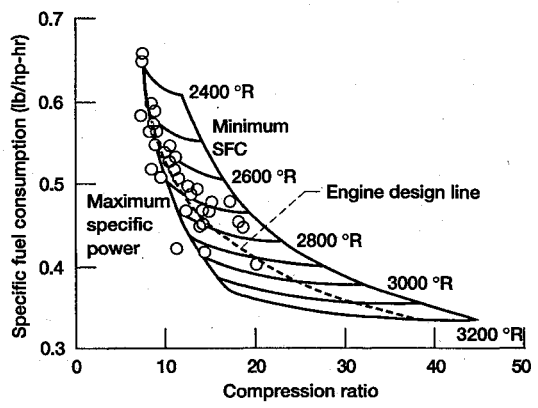

Fig. 5 Specific fuel consumption vs shaft compression ratio with turbine inlet temperature as a parameter, for gas turbine engines without a wave rotor topping cycle.

In Fig. 5, the specific fuel consumption of gas turbine engines without wave rotor topping cycles, as calculated with the simple model described previously, is plotted against compression ratio, with turbine inlet temperature as a parameter, for values of compression ratio between those for maximum specific power, and those for minimum specific fuel consumption. Also plotted are points (i.e., specific fuel consumption and compression ratio) for actual engines taken from Ref. 20. In addition, there is a line, called the engine design line, which is an approximately average line through the data, which will be taken as an appropriate line relating compression ratio and turbine inlet temperature for an average engine. Thus, for example, an engine with a compression ratio of 20 might be expected to have a turbine inlet temperature of 2900°R. Using this relationship between engine compression ratio and turbine inlet temperature, the specific power and specific fuel consumption were calculated for engines with, and without, a wave rotor topping cycle, using the wave rotor performance curve of Fig. 2. The results are plotted in Fig. 6. Again, at low values of shaft compression ratio, there is a significant gain; for a shaft compression ratio of 8, the addition of a wave rotor topping cycle increases the specific power by 19%, and reduces the specific fuel consumption by 16.2%. At higher values of shaft compression ratio, the advantage is lessened; for a shaft compression ratio of 40, addition of a wave rotor topping cycle increases specific power by 5.8%, and reduces specific fuel consumption by 5.6%. It is worth re-emphasizing that

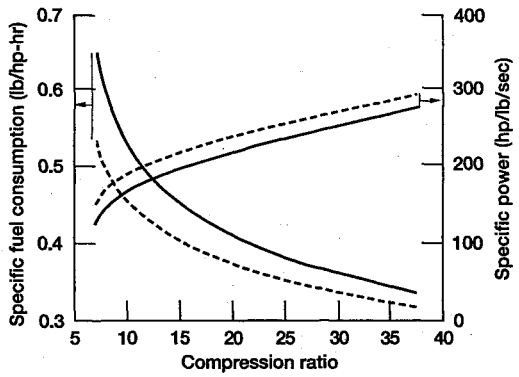

Fig. 6 Specific power and specific fuel consumption for engines with (----) and without (——) a wave rotor topping cycle. At any compression ratio, the basic engines are assumed to have turbine inlet temperatures corresponding to the design line of Fig. 5.

the previous results were derived using the wave rotor performance found experimentally.[11] This performance has been demonstrated, and therefore, it should be possible to obtain the calculated increases in specific power, and decreases in specific fuel consumption. However, the experimental rotor used in Ref. 11 was not optimized even for the experimental mass flow, and is certainly not optimum for any engine. It will be shown later that wave rotor performance can be optimized for a given mass flow, and the resulting performance will be better than that demonstrated by Klapproth et al.[11] Consequently, the increase in specific power, and reduction in specific fuel consumption that can be obtained by the use of an optimized wave rotor topping cycle, will also be greater. To perform this optimization, a model that can calculate wave rotor performance is required. Such a model is described in the next section.

CFD Wave Rotor Model

The computational wave rotor model is a one-dimensional code that follows a single wave rotor passage as it rotates past the various ports of the cycle. The working fluid is assumed to be a calorically perfect gas. The details of this code have been described in previous publications[15-17] and will not be presented here. Although several loss mechanisms are accounted for in the code, those of interest here result from the effects of viscosity, gradual passage opening (so-called finite opening time), and mixing of nonuniform velocity profiles in the exhaust port 4. It is assumed that the flow onto the rotor is at the correct angle to the axis so that the angle of incidence will be zero in the relative frame. If this is not the case, there will be an additional loss because of incidence.[9] The correct angle can be achieved either by mounting the duct at the appropriate angle, or by the use of guide vanes. Another loss that can arise in wave rotors is caused by mixing at the interface between air that has entered from the compressor and gas returning from the combustor. However, Keller and Chyou,[21] have indicated that this can be mitigated by proper design, and so it is not necessary to include this loss.

For reference, viscous effects are accounted for in the model with a source term in the governing momentum equation. The strength of the source term is determined by local velocity, density, and a constant friction factor that depends on the passage geometry. It is defined as[17]

$$f = 5.448(L/D_h)^{1.081}(\rho^* a^* L/\mu)^{-0.3953} \quad (1)$$

Since the viscosity does not change much with temperature, it is assumed constant at a value that is the average of ports 1 and 4. The hydraulic diameter is defined as

$$D_h = 2[bh/(b + h)] \quad (2)$$

The passage opening time is defined as

$$\tau_{ot} = ba^*/LR\omega \quad (3)$$

Increases in either finite opening time or friction factor result in decreased wave rotor performance. Furthermore, examination of Eqs. (1-3) reveals that, aside from an increase in rotor angular velocity, any reduction in the opening time increases the friction factor. For the purposes of this study the code was modified for use as a design rather than an analysis tool. In this capacity the prescribed inputs to the code are the friction factor, the ratio of specific heats, the passage opening time, the ratio of exhaust port to inlet port stagnation temperature T_4/T_1, and the so-called expansion ratio ε. The code then calculates the inlet stagnation pressures and temperatures, outlet static pressures, and port locations that ensure that the various waves are properly timed and that, upon completion of the cycle, the total mass flow from outlet ports matches the total flow to the inlet ports. Note that the code operates in the rotor frame of reference, and that as such, all stagnation properties discussed in this section of the article are to be understood as rotor relative. The balancing of mass flow also ensures that the passage completes the cycle in nearly the same state at which it began so that the cycle may start again. The calculation process is an iterative one with several subprocesses. These are shown in flowchart form in Fig. 7 and described briefly later. A complete calculated cycle, along with the port nomenclature, is shown in Fig. 8. This plot is a passage pressure contour with time (or circumferential position) and distance along the passage as the vertical and horizontal axes, respectively. Note that although the design code can calculate the appropriate port timing and relative stagnation conditions for all four ports in the cycle, only the inlet and exhaust portion of the cycle are used in this study and discussed in this article. The iteration begins at $\tau = 0$ with both ends of the passage closed and the gas in a state of uniform pressure and density and velocity ($u = 0$). The code then commences time integra-

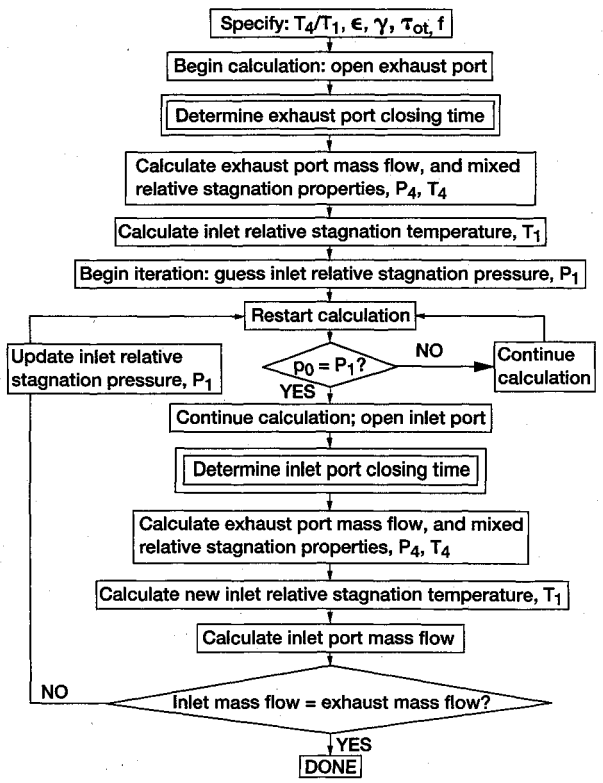

Fig. 7 Block diagram representation of the computational iteration for obtaining balanced port mass flow and proper placement of the exhaust and inlet ports.

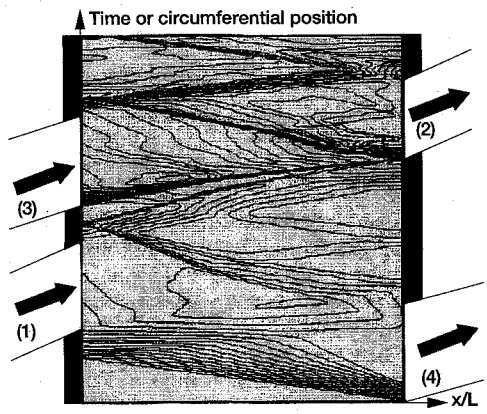

Fig. 8 Pressure contours for a properly timed four-port cycle.

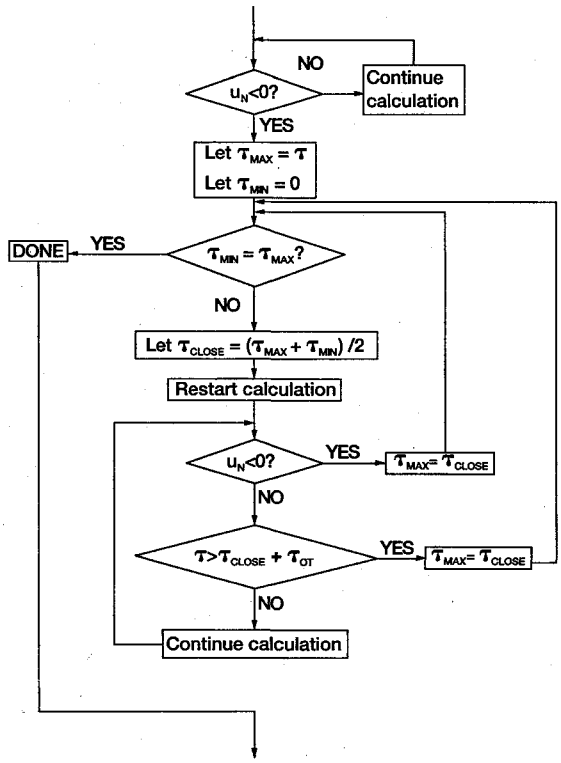

Fig. 9 Block diagram representation of the computational iteration for obtaining the exhaust port closing position.

tion with the opening of the exhaust port 4 (Fig. 7). Integration continues until the expansion fan, which was initiated by the exhaust port opening, reflects from the inlet side end-wall and returns to the exhaust port. When the expansion wave reaches the exhaust port, the outflow velocity begins to drop. Eventually, it drops below zero and inflow occurs. At this point the first subiteration begins (Fig. 9). This iteration locates the exhaust port closing time such that when the closing process is complete, the port velocity has just reached zero, thereby eliminating inflow. This closing time is then used for the remainder of the major iteration. Note that the opening of the inlet port, to be described later, alters the behavior of the exhaust expansion fan. This changes the time at which the exhaust velocity goes to zero; however, the alteration is generally very small, as is the error introduced. With the exhaust port timing set and the exhaust process complete, the exhaust mass flow and stagnation properties can be calculated. From the calculated value of T_4 and the specified value of T_4/T_1, the inlet temperature T_1 may be obtained. An initial guess at the inlet stagnation pressure P_1 is then made (i.e., $P_1 = P_4$), and the iteration restarts from $\tau = 0$. Integration continues until the pressure at the inlet

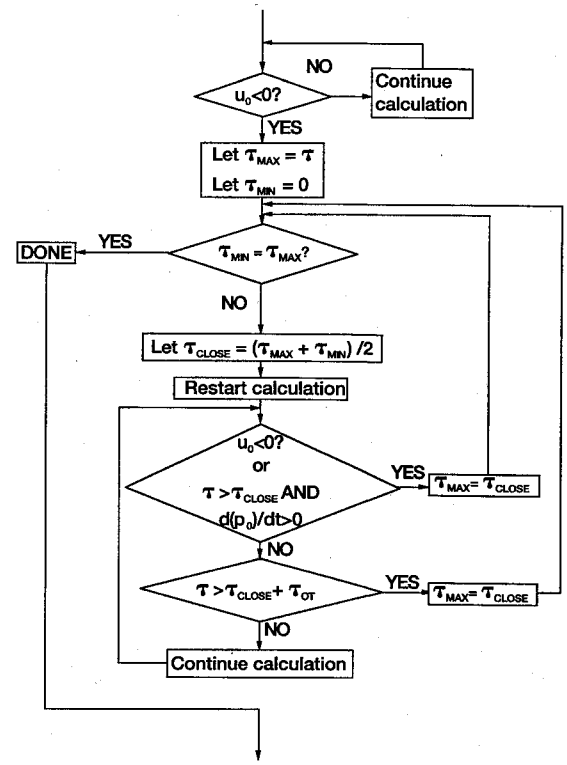

Fig. 10 Block diagram representation of the computational iteration for obtaining the inlet port closing position.

end of the passage, adjacent to the wall, matches P_1. At this point the inlet port is opened and the iteration continues until the flow in the inlet port reverses. Here, the second subiteration begins (Fig. 10). This process ensures that the inlet port completes the closing process just as the shock, which has coalesced from the compression wave caused by closing exhaust port 4, reaches the inlet end of the passage. The arrival of the shock is detected by either a sudden reversal of the inlet flow or a sudden change in passage pressure adjacent to the inlet. With the inlet closing complete, the inlet mass flow is known. This is compared to the exhaust mass flow. If they match, the iteration is complete, the correct port timing is known, and the ratio P_4/P_1 may be calculated. If not, a new guess is made for P_1 and the calculation is restarted. Once two guesses have been made for P_1, it may subsequently be updated using

$$P_1^{\text{new}} = P_1 - e[(P_1 - P_1^{\text{old}})/(e - e_{\text{old}})] \tag{4}$$

Optimization

Optimization means finding the wave rotor geometry (i.e., L, R, b, and h) plus rotational speed, which gives the best performance when used as the topping cycle for a particular engine. The wave rotor is required to handle the mass flow of the engine, at the temperature ratio T_4/T_1 of the engine. It will be assumed that leakage is negligible. There are two reasons for this assumption:

1) Recent experiments[22] at NASA Lewis Research Center have indicated that the effect of leakage on performance is negligible for values of G less than 0.01.

2) Work is in progress to develop seals to prevent, or significantly reduce, leakage. It is relatively easy to design for $G < 0.01$. It is also assumed that no cooling bleed flow is required from the wave rotor. In reality, since the highest pressure will, in fact, occur in the wave rotor, the optimization process will have to include bleed flow. Since the amount of bleed flow will vary from engine to engine, it was omitted here in the interest of simplicity.

It will be assumed that $\dot{m}$, Π_s, and T_4/T_1 are known for the engine. For most of the engines of interest, T_4/T_1 has a value

approximately equal to 2. The wave rotor expansion ratio giving the best performance depends on T_4/T_1. For T_4/T_1 close to 2, calculations have shown that the optimum value of the expansion ratio is approximately $\varepsilon = 0.4$. This value was assumed in the following calculations. Equating the engine mass flow to that of the wave rotor gives,

$$\dot{m} = \rho UA \tag{5}$$

where ρ and U are calculated at the wave rotor inlet port. In fact, ρ and U cannot be calculated at the inlet port, because they are set by the conditions in the wave rotor, and are found by solving the one-dimensional CFD code. Values of ρ and U are required to calculate the wave rotor geometry, which must be known to evaluate input parameters for the code. This dilemma is solved either by estimating the values for ρ and U, or using values from a previous solution, finding a solution with these values, and then using the new values from the solution to calculate new input. This is repeated until the input values are equal to the output values. The convergence is quite rapid; usually only three or four iterations are needed. Each of the n inlet ports has an area given by

$$A_n = \phi_{\text{in}} Rh = A/n \tag{6}$$

The value of ϕ_{in} comes from the cycle diagram (Fig. 8) for the particular value of T_4/T_1:

$$\phi_{\text{in}} = \tau_{\text{in}} 2\pi/\tau_{\text{cycle}} n \tag{7}$$

Thus, if a value of R is chosen, the value of h is determined via,

$$h = (\dot{m}/2\pi R\rho U)(\tau_{\text{cycle}}/\tau_{\text{in}}) \tag{8}$$

With h fixed, a value of b is assumed, which fixes the hydraulic diameter from Eq. (2). Given D_h, and assuming a value for L, the friction factor [Eq. (1)], and dimensionless passage opening time [Eq. (3)], can be calculated. One more quantity, the relative temperature ratio $(T_4/T_1)^{\text{rel}}$ is required for input into the code. As mentioned, the one-dimensional CFD code solves the unsteady flow within the rotor in the relative frame of the rotor. In this frame, the temperature ratio across the rotor will be different from the temperature ratio in the absolute frame. From the definition of relative stagnation temperature,[23] it follows that

$$T_1 = T_1^{\text{rel}} + (W^2/2c_{p1}) \tag{9}$$

$$T_4 = T_4^{\text{rel}} + (W^2/2c_{p4}) \tag{10}$$

The value of W depends on the rotor geometry, increasing with increasing R, but decreasing with increasing L:

$$W = \omega R = (2\pi a^* R/\tau_{\text{cycle}} Ln) \tag{11}$$

With W known, and knowing the value of T_4/T_1 required, it is possible to find the value of $(T_4/T_1)^{\text{rel}}$. The value of $(T_4/T_1)^{\text{rel}}$ is used in the CFD code to solve for $(P_4/P_1)^{\text{rel}}$, which is then corrected to the absolute value via the isentropic relationship:

$$(P_4/P_1)/(P_4/P_1)^{\text{rel}} = [(T_4/T_1)/(T_4/T_1)^{\text{rel}}]^{\gamma/(\gamma-1)} \tag{12}$$

Large values of W are undesirable, since then the absolute performance drops significantly.

The optimization procedure is as follows: for given values of mass flow, and absolute temperature ratio T_4/T_1, corresponding to the engine selected, values of n, L, and R are picked, thereby determining h. The absolute performance is calculated for various values of b. At small values of b, the opening time is small, but the friction factor is high, reducing performance.

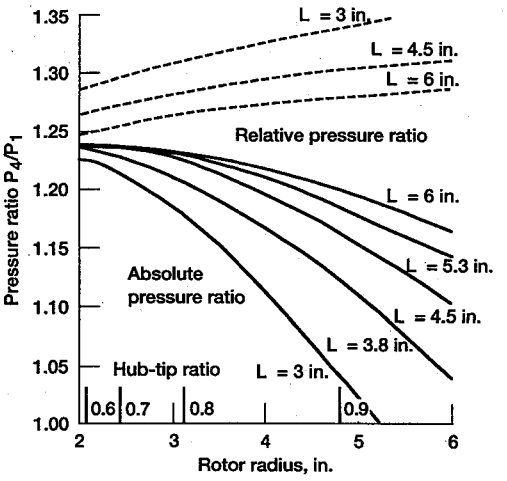

Fig. 11 Relative and absolute wave rotor pressure ratio vs length and radius for wave rotors sized for a mass flow of 4 lbm/s. The passage width has been optimized at each radius and length.

At large values of b, friction is low, but the large opening time reduces performance. There is an optimum value of b in between, which is selected. This calculation is repeated at different values of R, for the same value of L. Then a new value of L is chosen, and the process is repeated. The performance optimized with respect to b, at each value of R, is plotted in Fig. 11 for $n = 2$, and a mass flow of 4 lb/s. The relative performance is also shown in Fig. 11. At small values of R, the value of W is low, and the absolute performance approaches the relative performance, whereas at large values of R, there is significant difference between the two. Large values of L reduce ω, and therefore W, but also increase the friction factor, reducing performance. From this plot, values of L and R, and thus b and h, can be selected that will give optimum performance. For the case shown, these values are $L = 5.25$ in., $R = 2.5$ in., $h = 0.83$ in., and $b = 0.28$ in.

Application to Different Engines

Using the methodology previously outlined, the dimensions of optimal wave rotors can be found for gas turbine engines of various sizes. Such calculations have been made for hypothetical engines of small (4 lb/s), medium (26 lb/s), and large (400 lb/s) engines. For these engines, typical values of compression ratio and turbine inlet temperature were selected, as well as estimates of the engine dimensions. The values are

Table 1 Optimized wave rotor specification

	Small	Medium	Large
Engine			
Core mass flow, lbm/s	4	25	400
Shaft compression ratio	7	8	40
Turbine inlet temperature, °R	2,400	2,400	3,200
Diameter, in.	24	24	50
Length, in.	40	48	190
Wave rotor			
Diameter, in.	6	11	24
Length, in.	6	12	12
Passage height, in.	0.673	2.50	4.51
Passage width, in.	0.30	0.48	0.38
Rotor speed, rpm	15,600	7,700	4,200
T_4/T_1	2.3	2.3	1.9
P_4/P_1	1.232	1.272	1.204
Performance			
Untopped spectral power, hp/lbm/s	121	151	276
Topped spectral power, hp/lbm/s	149	183	300
% increase from wave rotor	23	21	8.7
Untopped SFC, lbm/hp/h	0.650	0.529	0.338
Topped SFC, lbm/hp/h	0.528	0.436	0.311
% decrease from wave rotor	18.8	17.5	8.0

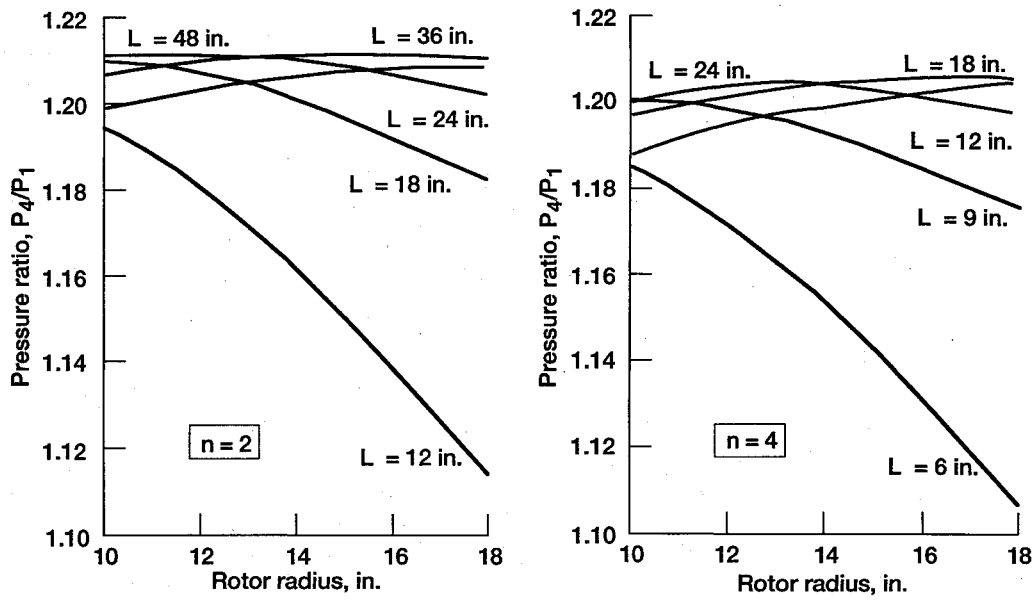

Fig. 12 Absolute pressure ratio vs length and radius for wave rotors sized for a mass flow of 400 lbm/s. Curves are given for two wave rotor cycles per revolution (n = 2) and for four wave rotor cycles per revolution (n = 4).

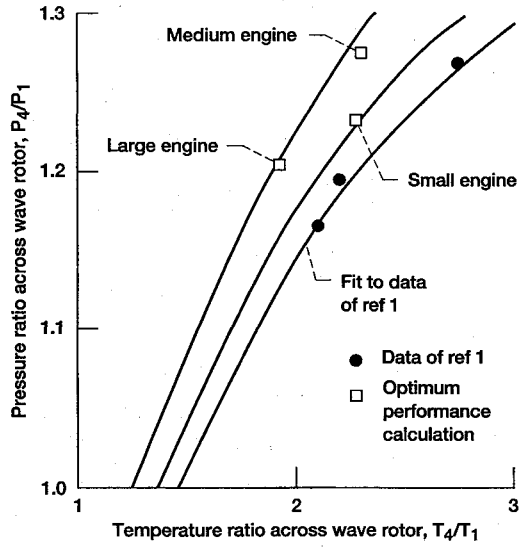

Fig. 13 Performance of wave rotors optimized for the small, medium, and large engines together with the performance of the wave rotor measured by Klapproth et al.[11]

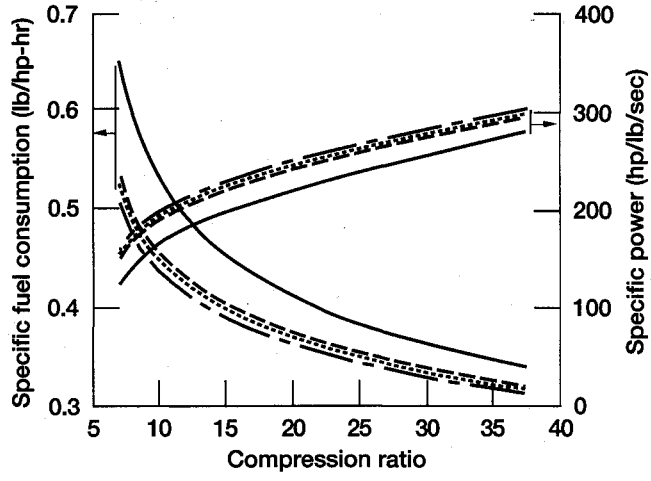

Fig. 14 Improvement in gas turbine engine performance that can be obtained with a wave rotor topping cycle employing wave rotors of differing performance, for engines corresponding to the engine design line. Shown are curves for engines with no topping stage (——), and engines with topping cycles using rotors with the performance of Ref. 1 (– – –), with the performance optimized for a small engine (· · · ·), and with the performance optimized for a large engine (— — —).

listed in Table 1. Also listed are the dimensions and performance of the optimal wave rotor for each engine. It will be seen that the wave rotor can be relatively small compared with the engine itself.

In one sense, there is not, in fact, an optimum wave rotor at all! This is because there is an optimum for each value of n, the number of cycles per revolution. Although the highest performance comes from n = 1, the change in performance as n is increased is very small. On the other hand, the length of the optimum rotor scales almost inversely with n. This is illustrated in Fig. 12, showing performance curves for the large engine for n = 2 and 4. There is almost no change in performance, but the length of the optimal n = 4 rotor is half that of the n = 2 rotor. From a size point of view, the n = 4 rotor seems preferable. However, the higher value of n leads to much more ducting, which could be a severe complication. In Table 1, it was assumed that n = 2 would be appropriate for the small and medium engines, but that n = 4 would be more appropriate for the large engine. Obviously, for a real engine, the choice of n will be made by the engine designer based on engineering considerations. Another complication is indicated in Fig. 11, in which approximate values of the wave rotor hub–tip ratio are given. Performance optimization for the small engine drives the choice of wave rotor radius to small values, which results in low values of the hub–tip ratio. The one-dimensional code does not presently account for hub–tip ratio effects. Consequently, the lower limit of hub–tip ratio for a wave rotor is not known. Modification of the code is required to include this effect. Turbomachinery typically has a lower limit of hub–tip ratio of 0.7. It seems reasonable to use a similar criterion for wave rotors also, and this may limit the value of radius used.

The calculated performance of the three optimal wave rotors has been plotted in Fig. 13. It is seen that each wave rotor is predicted to give a performance better than that of the wave rotor of Ref. 11. This is reflected in the wave rotor enhanced performance of the three hypothetical engines, as listed in Table 1. All three engines will give a better performance than that indicated by the calculation based on the wave rotor performance of Ref. 11, increasing the specific power another

2.3% for the small engine, 3.1% for the medium engine, and 2.7% for the large engine, and reducing the specific fuel consumption a further 1.6% for the small engine, 2.6% for the medium engine, and 2.4% for the large engine. The increase in specific power, and reduction in specific fuel consumption that can be expected for engines corresponding to the engine design line of Fig. 5, when enhanced by wave rotors optimized for the small and large engines, is indicated in Fig. 14.

Summary and Conclusions

The advantages of using a wave rotor topping cycle on a gas turbine engine have been reviewed. A one-dimensional, experimentally validated, CFD model for the calculation of wave rotor performance has been described briefly. This model was used to find optimally sized wave rotors for three hypothetical engines. It is concluded that the use of a wave rotor topping cycle on a gas turbine engine can do the following:

1) Based on demonstrated wave rotor performance, the cycle gives increases in a specific power of 19.2% at a compression ratio of 8, a turbine inlet temperature of 2400°R, and 5.8% at a compression ratio of 40, and a turbine inlet temperature of 3200°R.

2) Based on demonstrated wave rotor performance, the cycle gives reductions in a specific fuel consumption of 16.2% at a compression ratio of 8, a turbine inlet temperature of 2400°R, and 5.6% at a compression ratio of 40, and a turbine inlet temperature of 3200°R.

3) With optimally sized wave rotors, the cycle gives increases in a specific power of 21% at a compression ratio of 8, a turbine inlet temperature of 2400°R, and 8.7% at a compression ratio of 40, and a turbine inlet temperature of 3200°R.

4) With optimally sized wave rotors, the cycle gives reductions in a specific fuel consumption of 17.5% at a shaft compression ratio of 8, a turbine inlet temperature of 2400°R, and 8% at a shaft compression ratio of 40, and a turbine inlet temperature of 3200°R. In addition, optimal wave rotors are reasonably sized for this application.

References

[1]Meyer, A., "Recent Developments in Gas Turbines," *Mechanical Engineering*, Vol. 69, No. 4, 1947, pp. 273–277.

[2]Kollbrunner, T. A., "Comprex Supercharging for Passenger Diesel Car Engines," West Coast International Meeting, Society of Automotive Engineers Paper 800884, Los Angeles, CA, Aug. 1980.

[3]Jenny, E., and Zumstein, B., *Pressure Wave Supercharging of Passenger Car Diesel Engines*, Inst. of Mechanical Engineers, CP C-44, 1982, pp. 129–141.

[4]Croes, N., "The Principle of the Pressure-Wave Machine as Used for Charging Diesel Engines," *Shock Tube and Shock Wave Research: Proceedings of the 11th International Symposium on Shock Tubes and Waves*, edited by B. Ahlborn, A. Hertzberg, and D. Russell, Univ. of Washington Press, Seattle, WA, 1978, pp. 36–55.

[5]Keller, J. J., "Some Fundamentals of the Supercharger Comprex," *Machinery for Direct Fluid-Fluid Energy Exchangers*, edited by J. F. Sladsky Jr., American Society of Mechanical Engineers AD-07, New York, 1984, pp. 47–54.

[6]Weatherston, R. C., Smith W. E., Russo, A. L., and Marrone, P. V., "Gasdynamics of a Wave Superheater Facility for Hypersonic Research and Development," Cornell Aeronautical Lab., Rept. AD-188-A-1, Buffalo, NY, 1959.

[7]Kentfield, J. A. C., "Nonsteady, One-Dimensional, Internal, Compressible Flows," Oxford Univ. Press, New York, 1993, pp. 161–163.

[8]Pearson, R. D., "Pressure Exchangers and Pressure Exchange Engines," *Thermodynamics and Gas Dynamics of Internal Combustion Engines*, edited by D. E. Winterbone and S. C. Low, Oxford Univ. Press, New York, 1982, pp. 903–943.

[9]Weber, H. E., *Shock Wave Engine Design*, Wiley, New York, 1995.

[10]Zauner, E., Chyou, Y.-P., Walraven, F., and Althaus, R., "Gas Turbine Topping Stage Based on Energy Exchangers: Process and Performance," American Society of Mechanical Engineers Paper 93-GT-58, May 1993.

[11]Klapproth, J. F., Perugi, A., Gruszczynski, J. S., Stoffer, L. J., and Alsworth, C. C., "A Brief Review of the G.E. Wave Rotor Program (1958–1963)," *Proceedings of the 1985 ONR/NAVAIR Wave Rotor Research and Technology Workshop*, Naval Postgraduate School, Rept. NPS-67-85-008, Monterey, CA, 1985, pp. 172–193.

[12]Ruffles, P., "Rolls-Royce Study of Wave Rotors 1965–1970," *Proceedings of the 1985 ONR/NAVAIR Wave Rotor Research and Technology Workshop*, Naval Postgraduate School, Rept. NPS-67-85-008, Monterey, CA, 1985, pp. 116–124.

[13]Nalim, R., "Preliminary Assessment of Combustion Modes for Internal Combustion Wave Rotors," AIAA Paper 95-2801, July 1995.

[14]Wilson, J., and Paxson, D. E., "Jet Engine Performance Enhancement Through Use of a Wave-Rotor Topping Cycle," NASA TM 4486, Oct. 1993.

[15]Paxson, D. E., "A General Numerical Model for Wave Rotor Analysis," NASA TM 105740, July 1992.

[16]Paxson, D. E., "Comparison Between Numerically Modeled and Experimentally Measured Loss Mechanisms in Wave Rotors," *Journal of Propulsion and Power*, Vol. 11, No. 5, 1995, pp. 908–914.

[17]Paxson, D. E., and Wilson, J., "Recent Improvements to and Validation of the One Dimensional NASA Wave Rotor Model," NASA TM 106913, May 1995.

[18]Kentfield, J. A. C., "The Performance of Pressure Exchanger Equalizers and Dividers," *Journal of Basic Engineering*, Vol. 91, No. 3, 1969, pp. 361–370.

[19]Mattingly, J. D., Heiser, W. H., and Daley, D. H., *Aircraft Engine Design*, AIAA Education Series, AIAA, Washington, DC, 1987.

[20]Anon., "Specifications, U.S. Gas Turbine Engines," *Aviation Week and Space Technology*, March 19, 1990, p. 165.

[21]Keller, J. J., and Chou, Y.-P., "On the Hydraulic Lock-Exchange Problem," *Journal of Applied Mathematics and Physics (ZAMP)*, Vol. 42, No. 6, 1991, pp. 874–910.

[22]Wilson, J., and Fronek, D., "Initial Results from the NASA-Lewis Wave Rotor Experiment," AIAA Paper 93-2521, June 1993.

[23]Glassman, A. J. (ed.), "Turbine Design and Application," NASA SP-290, 1994.